Biotechnology and Bioengineering

WILEY

BIOTECHNOLOGY BIOENGINEERING

ARTICLE OPEN ACCESS

All You Can Eat Yeast: Substituting Hexose Transporters With *AtSWEET7* Alleviates Glucose Repression, Enabling Simultaneous Utilization of Sugars in Renewable Feedstocks

Nurzhan Kuanyshev[1,2] | Degaulle Dai[1,2,3] | Jungyeon Kim[4] | Nam Kyu Kang[5] | Ming-Hsun Cheng[6] | Vijay Singh[2,7] | Yong-Su Jin[1,2,3]

[1]Carl R. Woese Institute for Genomic Biology, University of Illinois at Urbana–Champaign, Urbana, Illinois, USA | [2]DOE Center for Advanced Bioenergy and Bioproducts Innovation, University of Illinois Urbana–Champaign, Urbana, Illinois, USA | [3]Department of Food Science and Human Nutrition, University of Illinois at Urbana–Champaign, Urbana, Illinois, USA | [4]Graduate School of International Agricultural Technology, Seoul National University, Pyeongchang-gun, Gangwon-do, Republic of Korea | [5]Department of Chemical Engineering, Kyung Hee University, Yongin-si, Gyeonggi-do, Republic of Korea | [6]Department of Natural Resources and Society, University of Idaho, Idaho Falls, Idaho, USA | [7]Department of Agricultural and Biological Engineering, University of Illinois at Urbana–Champaign, Urbana, Illinois, USA

Correspondence: Yong-Su Jin (ysjin@illinois.edu)

Received: 18 November 2025 | **Revised:** 27 February 2026 | **Accepted:** 28 February 2026

Funding: DOE Center for Advanced Bioenergy and Bioproducts Innovation U.S. Department of Energy, Office of Science, Office of Biological and Environmental Research, Grant/Award Number: DE-SC0018420

Keywords: hexose | lignocellulose | sugar transport | SWEET | xylitol | xylose | yeast

ABSTRACT

Yeast sugar transporters have highly evolved for preferential glucose transport, a significant roadblock for utilizing non-glucose sugars in renewable feedstocks such as lignocellulosic biomass. To enable simultaneous transport of multiple sugars, native hexose transporters were replaced by SWEET7p from *Arabidopsis thaliana* in engineered *Saccharomyces cerevisiae* capable of fermenting xylose. Engineered *S. cerevisiae* exhibited reduced glucose preference, simultaneously co-fermenting glucose, mannose, fructose, and xylose both in synthetic and industrial media. Continuous culture experiments demonstrated the co-consuming phenotype and alleviation of glucose repression by engineered *S. cerevisiae*. In addition to hexose and pentose, the NKSW7-1 strain consumed xylitol as a carbon source. Through transcriptomic and metabolomic analysis of the NKSW7-1 strain, we show that the replacement of *HXT1-7* with *AtSWEET7* led to systemwide reprogramming of the central carbon metabolism. This broad transport capacity of AtSWEET7p holds promise for achieving co-consumption of all sugars in underutilized renewable feedstocks by microbial cell factory.

1 | Introduction

Greenhouse gas emission from fossil fuel utilization is a critical target in combating climate change and environmental pollution (Clomburg et al. 2017; Robertson et al. 2017). Consequently, modern energy and chemical industries have focused on more sustainable and lower-emission processes. To this end, microbial fermentation of renewable biomass such as lignocellulosic plant materials could enable more sustainable production of biofuels and biochemicals, serving as an effective substitute for conventional petrochemical processes (Bokinsky et al. 2011; Steen et al. 2010).

In the process of producing sugar cane juice, substantial amounts of byproduct are generated in the form of

This is an open access article under the terms of the Creative Commons Attribution License, which permits use, distribution and reproduction in any medium, provided the original work is properly cited.

© 2026 The Author(s). *Biotechnology and Bioengineering* published by Wiley Periodicals LLC.

lignocellulosic waste, commonly referred as sugarcane bagasse (SCB) (Thite and Nerurkar 2019). SCB is composed of approximately 41.2% glucans and 28.2% xylan, along with other constituents. The hydrolysis of SCB into simple sugars can enable further bioconversion of the byproduct. In addition to the SCB hydrolysate, lignocellulosic hydrolysates from plant cell walls contain hexose and pentose sugars, primarily represented by glucose and xylose (Jönsson et al. 2013). Therefore, to develop a more efficient and rapid conversion process of plant cell walls into target commercial products, both hexose and pentose sugars need to be simultaneously converted into products by engineered microbial hosts (Jin et al. 2003; Kim et al. 2012). The widely used industrial fermentation host *Saccharomyces cerevisiae* lacks a native xylose utilization pathway, so it has been extensively engineered to utilize xylose (Kim et al. 2013; Lee et al. 2021). Even so, these engineered strains still retain a preference toward consumption of glucose over xylose (Carroll and Somerville 2009; Subtil and Boles 2012). Glucose repression of uptake of xylose and other monosaccharides by native hexose transporters is considered a main bottleneck, limiting simultaneous utilization of glucose and other sugars (Gárdonyi et al. 2003; Hamacher et al. 2002; Parachin et al. 2011; Sedlak and Ho 2004).

Application of the oxido-reductase pathway to assimilate xylose results in production of xylitol, an undesirable by-product (Kim et al. 2013). Because *S. cerevisiae* also lacks a native transport capacity of xylitol, accumulated xylitol is rendered unusable. Many transporter engineering studies on both heterologous and endogenous sugar transporters have examined the feasibility of rewiring *S. cerevisiae* glucose preference (Farwick et al. 2014; Hou et al. 2017; Li et al. 2016; Nijland and Driessen. 2019; Reider Apel et al. 2016; Shin et al. 2015; Young et al. 2014), but the xylitol reassimilation problem was comparatively overlooked, with a limited number of studies addressing it (Jordan et al. 2016; Tani et al. 2017). While prior studies lent some insight into the molecular basis of yeast sugar transporter preferences, implementation of newly identified transporters for simultaneous conversion of mixed sugars has been limited because of endogenous transporter tendencies to override heterologous transporter capacity.

The SWEET (Sugar Will Eventually be Exported Transporters) superfamily is ubiquitous in plant genomes but is not expressed by most fungi (Jeena et al. 2019; Seppälä et al. 2016; Xue et al. 2022). Yeast engineering involving SWEET transporters has recently been applied toward mixed sugar co-fermentation (Kuanyshev et al. 2021a; Podolsky et al. 2021). Podolsky et al. demonstrated functional expression of an anaerobic fungal (*Neocallimastigomycota*) SWEET transporter in *S. cerevisiae*. They further improved SWEET sugar co-transport efficiency through the creation of chimera proteins. However, both the native SWEET and its chimeras showed weak co-fermentation capability, consuming only 20 g/L each of 30 g/L glucose and 25 g/L xylose in 120 h. Comparatively, the parental strain with native hexose transporters consumed 40 g/L of either sugar within 48 h (Podolsky et al. 2021). In addition, our previous work showed that *AtSWEET7* can be functionally expressed in *S. cerevisiae*, enabling simultaneous co-consumption of glucose and xylose. Moreover, *AtSWEET7* did not exhibit glucose-based sugar transport inhibition in this mixed substrate (Kuanyshev et al. 2021a).

This potential for simultaneous hexose and pentose sugar fermentation could enable the conversion of lignocellulosic biomass to industrial bioproducts and biofuels using a continuous fermentation process. During the continuous fermentation, products are generated at a constant rate and fermentation downtime between batches that would occur in batch or fed-batch fermentations is avoided. Consequently, continuous fermentation holds advantages over batch and fed-batch fermentation through the usage of smaller fermenters, lower equipment and operation costs, faster production of products, and reduction of unwanted byproducts (Brethauer and Wyman 2010; Cysewski and Wilke 1978; Palmqvist and Hahn-Hägerdal 2000).

Sugar transport in *S. cerevisiae* is facilitated by actively expressed hexose transporters (*HXT1-7* and *GAL2*) with *HXT8–HXT17* being either inactive (not transcribed) or cryptic (Hamacher et al. 2002; Özcan and Johnston 1999; Sedlak and Ho 2004). In this study, we systematically replaced the Hxt1-7p and Gal2p transporters in a highly optimized xylose-consuming *S. cerevisiae* strain with *Arabidopsis thaliana* AtSWEET7p to construct an engineered yeast strain with multisugar utilization capacity (Tsai et al. 2015). We investigated the sugar fermentation profiles of this *AtSWEET7* integrated strain using different sugar combinations. To further show the applicability of this strain in industrial conditions, we performed bagasse hydrolysate and sugarcane juice fermentations, as well as continuous multi-sugar fermentations. Remarkably, we discovered that *AtSWEET7* has the capacity to transport xylitol, an additional advantage toward reducing byproduct accumulation in industrial use cases. Finally, the transcriptional and metabolic effects of the major hexose substitution were elucidated through RNA sequencing and metabolomics. In this study, we demonstrate the ability of this engineered *S. cerevisiae* to utilize four sugars simultaneously, transport xylitol, and show the industrial potential of the AtSWEET7p transporter as a versatile multisugar transporter, especially under continuous culture conditions.

2 | Results

2.1 | Expression of *AtSWEET7* in Engineered *S. cerevisiae* Conferred Co-Consumption of Major Hexoses and Pentoses

In our previous study, *AtSWEET7* was identified as a sugar transporter capable of transporting glucose and xylose simultaneously when expressed in the *hxt* null *S. cerevisiae* SR8D8 (HXT1-7 Δ/GAL2Δ) strain using a multi-copy plasmid (Kuanyshev et al. 2021a). Similarly to the previous study, we used the *hxt* null *S. cerevisiae* SR8D8 strain that unable to grow on any sugars, to evaluate effects of *AtSWEET7* copy number on glucose and xylose consumption rates in engineered *S. cerevisiae* We integrated one to three copies of *AtSWEET7* under a constitutive promoter into the *hxt* null *S. cerevisiae* SR8D8 strain and observed substantial improvements in glucose uptake rates by increasing the copy number of *AtSWEET7* (1, 1.49, and 1.66 g/L · h for one, two, and three copies, respectively). However, xylose uptake rates did not change with increased copy numbers (Supporting Information Figure 1).

Next, we integrated multiple copies of *AtSWEET7* into a highly optimized xylose-fermenting *S. cerevisiae* strain (CT2) (Tsai et al. 2015). Activities of endogenous Hxt1-7p transporters confer preferred glucose consumption in *S. cerevisiae* when mixtures of glucose and xylose are provided. Therefore, the deletion of endogenous sugar transporters (*HXT1-7* and *GAL2*) and high-copy expression of *AtSWEET7* is necessary to achieve simultaneous co-fermentation of glucose and xylose. We replaced *HXT1-7* and *GAL2* with *AtSWEET7* in the CT2 strain, substituting coding sequences only under the control of native promoters (Figure 1A), resulting in the construction of the NKSW7-1 strain. While this would theoretically increase *AtSWEET7* copy number to up to 8, depending on external glucose levels, only four copies of integrated *AtSWEET7* under the control of *HXT2*, *HXT4*, *HXT7*, and *GAL2* promoters were highly expressed due to the native glucose-sensing mechanism that modulates the expression levels of sugar transporters in *S. cerevisiae* (Özcan and Johnston 1999). When sugar consumption rates of the NKSW7-1 strain were examined under hexose (glucose, fructose, and mannose) and pentose (xylose) conditions (Supporting Information Figure 2). The NKSW7-1 strain exhibited 2.15, 1.15, and 1.2 g/L · h consumption rates for glucose, mannose, and fructose, respectively. These are 62%, 50%, and 45% slower as compared to glucose, mannose, and fructose consumption rates (3.45, 2.3, and 2.64 g/L · h) of the CT2 strain. The xylose utilization rate of the NKSW7-1 strain, however, was similar to that (~1.4 g/L/h) of the CT2 strain.

2.2 | *AtSWEET7* Expression Enables Dual Sugar Co-Utilization of Hexose/Pentose Combinations

The NKSW7-1 strain was capable of growing on media containing hexose sugars (glucose, fructose, and mannose) and the pentose sugar xylose as sole carbon sources, although its growth rates were slower compared to its parental strain, CT2. When provided with a mixture of glucose, fructose, mannose, and xylose, CT2 demonstrated a clear preference for glucose, consuming it before other sugars (fructose, mannose, and xylose). In case of hexose (glucose, fructose, and mannose) and xylose mixture condition, the CT2 strain consumed hexose (glucose, fructose, and mannose) first at the at rate of ~ 2.6 g/L · h, following which xylose was consumed at the rates of 0.79, 0.61, and 1.28 g/L · h for fructose-xylose, mannose-xylose, and glucose-xylose mixtures, respectively (Supporting Information Figure 3). Under conditions when glucose was present alongside other hexoses (mannose or fructose), CT2 preferentially consumed glucose at a rate of 2.2 g/L · h. Mannose and fructose were utilized only after glucose depletion, at rates of 1.57 and 1.38 g/L · h, respectively (Supporting Information Figure 4). The CT2 strain only displayed co-utilization of mannose with fructose at the rates of 2 and 1.5 g/L · h, respectively, with a slight preference toward fructose. On the other hand, the NKSW7-1 strain showed co-utilization of dual sugars regardless of combination, at an average consumption rate of 1.1 ± 0.3 g/L · h (Supporting Information Figures 3 and 4).

2.3 | *AtSWEET7* Expression Enables Simultaneous Multi-Sugar and Sugar Alcohol Transport

Dual sugar fermentation experiments clearly demonstrated the advantage of *AtSWEET7* expression in enabling multi-sugar co-utilization in *S. cerevisiae* over native *HXT1-7* and *GAL2*. Next, we performed a quadruple sugar fermentation using 20 g/L each of glucose, fructose, mannose, and xylose. As expected, CT2 consumed sugars sequentially, with glucose being consumed first at a rate of 1.9 g/L · h, then fructose and mannose at a rate of 1.38 g/L · h, and finally xylose at a rate of 0.61 g/L · h (Figure 1B). These results once again demonstrate the sequential consumption of glucose, then other hexose sugars, and then

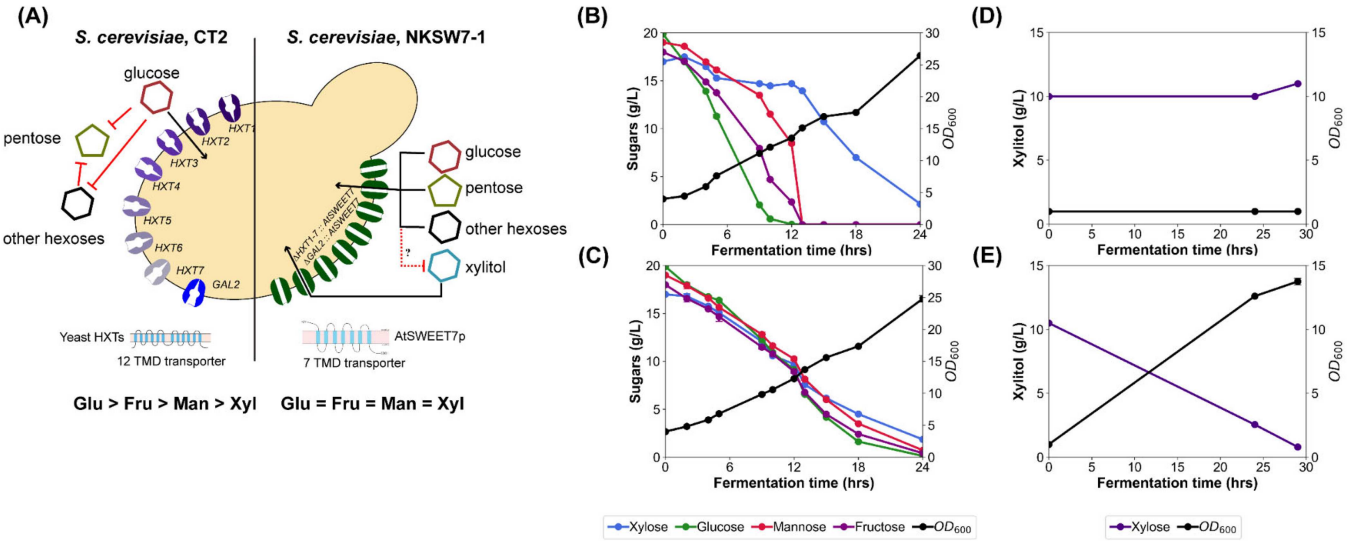

FIGURE 1 | Comparison of CT2 and engineered NKSW7-1 strains. (A) In CT2 main hexose transporters HXT1-7p have high preference toward glucose transport. By expressing AtSWEET7p in the place of endogenous transporters we can enable simultaneous co-fermentation of glucose, xylose, and other monosaccharides. In addition, AtSWEET7p enables utilization of xylitol, however it needs to be determined whether other sugars would inhibit or allow co-transport of xylitol TMD – transmembrane domain. (B, C) Quadruple sugar flask fermentation profile of CT2 and NKSW7-1. (D, E) Xylitol fermentation as a sole carbon source by CT2 and NKSW7-1. Values are means of two independent experiments, and error bars indicate standard error.

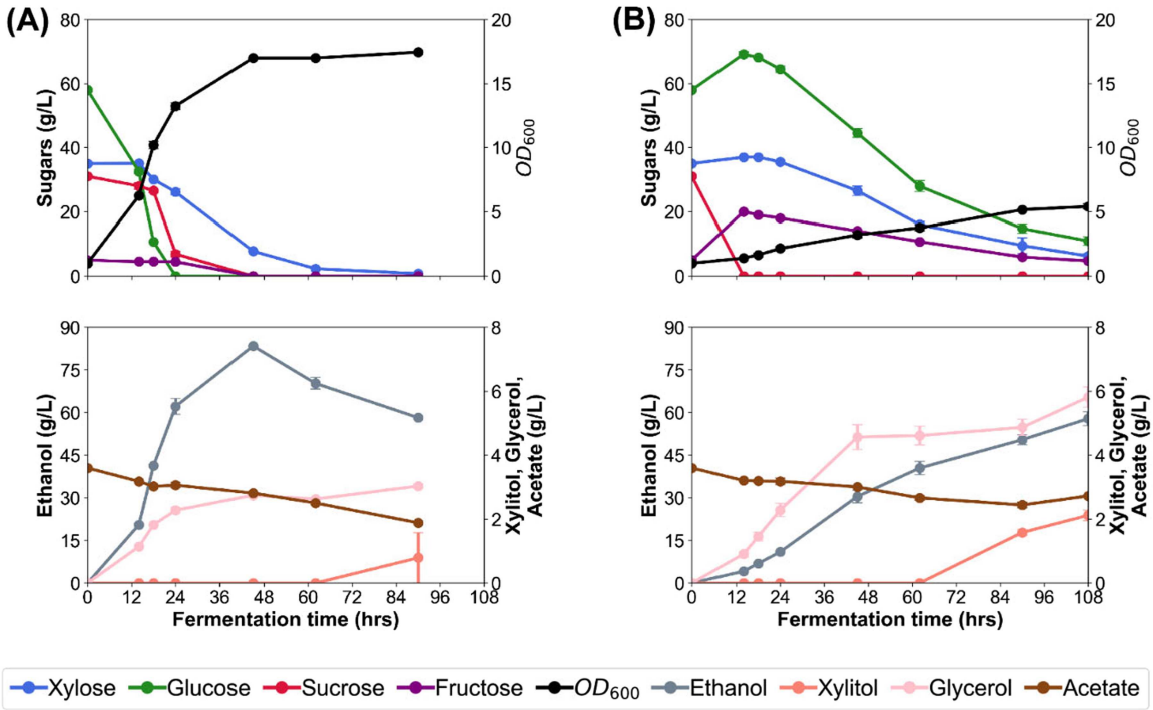

FIGURE 2 | Bagasse hydrolysate (BH) and sugar cane juice (SCJ) mixture flask fermentation profile. (A) Fermentation and growth profile of CT2 and (B) NKSW7-1. Cells were precultured in 50% BH with 1xYP until mid-exponential phase. For the main fermentation cells were washed 2x in deionized water and inoculated into 50% BH, 25% SCJ, and 1xYP media at OD_{600} 1 and pH 6. Cells were incubated at 100 rpm and 30°C. Values are means of two independent experiments, and error bars indicate standard error.

the pentose xylose by the endogenous *S. cerevisiae* transport system. In contrast, NKSW7-1 exhibited simultaneous co-fermentation of all sugars at a rate of 0.73 ± 0.08 g/L·h (Figure 1C). It is well-known that trace amounts of xylitol are secreted by engineered *S. cerevisiae* during xylose fermentation. *S. cerevisiae* does not have dedicated polyol transporters and relies on hexose transporters to reassimilate xylitol, and xylitol re-assimilation requires extended incubation times (Jeffries and Jin 2004; Jin et al. 2003; Jordan et al. 2016; Toivari et al. 2004). While the amounts of xylitol produced by engineered *S. cerevisiae* are not substantial, at the industrial scale accumulation becomes economically relevant. Therefore, upon confirming the wide substrate range of *AtSWEET7*, we investigated the xylitol consumption capability of NKSW7-1. Our experiments demonstrated that in contrast to CT2, which cannot consume xylitol, the NKSW7-1 strain was able to rapidly consume xylitol as a sole carbon source during flask fermentation at a rate of 0.33 g/L · h (Figure 1D,E).

2.4 | Bagasse Hydrolysate Sugars Are Efficiently Co-Fermented by NKSW7-1

Most yeast strains used in sugarcane fermentation are unable to utilize all sugars simultaneously and/or can only utilize hexose sugars, a relevant shortcoming considering the high proportion of glucose and xylose in SCB (Thite and Nerurkar 2019). To show the applicability of *AtSWEET7* in solving this, we performed a bagasse hydrolysate fermentation using CT2 and NKSW7-1, with the principal goal of investigating NKSW7-1 behavior in an industrial feedstock containing not only sugars but also inhibitors such as acetate and other compounds. As expected, CT2 consumed glucose and xylose in a sequential manner as demonstrated in a synthetic medium (Supporting Information Figure 5A). All sugars were consumed within 85 h with a total sugar consumption rate of 1.19 g/L · h and a specific sugar consumption rate of 0.06 g/L · h/OD_{600}. Upon glucose depletion, CT2 co-consumed xylose and acetate, consuming a total of 2.34 g/L of acetate (Supporting Information Figure 5A). In sharp contrast to CT2, NKSW7-1 showed simultaneous co-consumption of glucose and xylose, albeit at a slower rate than CT2, with a total sugar consumption rate of 1.01 g/L · h (glucose consumption rate of 0.63 g/L · h and xylose consumption rate of 0.38 g/L · h) and a specific sugar consumption rate of 0.096 g/L · h/OD_{600} (Supporting Information Figure 5B). Remarkably, NKSW7-1 was able to co-consume 2 g/L of acetate even in the presence of substantial amounts of glucose, indicating *AtSWEET7* expression decreases glucose repression of acetate utilization (Supporting Information Figure 5B). While the overall NKSW7-1 fermentation was slower for CT2, the specific consumption rate of each sugar by NKSW7-1 was higher than by CT2.

2.5 | NKSW7-1 Exhibits High Invertase Activity, Rapidly Hydrolyzing Sucrose

We performed fermentation experiments using mixtures of a sugar cane juice and a bagasse hydrolysate to demonstrate simultaneous sugar co-consumption by NKSW7-1 of an industrial sugar cane feedstock. As expected, CT2 exhibited a glucose repression phenotype, with sequential utilization of glucose, sucrose, and xylose. All sugars were consumed within 90 h (Figure 2A). In contrast, NKSW7-1 simultaneously co-

fermented glucose, fructose, and xylose within 110 h (Figure 2B). NKSW7-1 also unexpectedly rapidly converted all sucrose to corresponding monosaccharides within 12 h, indicating increased invertase secretion by the strain. Although NKSW7-1 was superior in terms of specific consumption rate (0.182 g/L · h/OD_{600} vs. 0.078 g/L · h/OD_{600}), it is still inferior to CT2 in terms of ethanol productivity and individual sugar consumption rate (Figure 2). However, the unique co-consuming phenotype of NKSW7-1 affords advantages in continuous fermentation, regardless of kinetic inferiority, as will be described hereafter.

2.6 | NKSW7-1 Achieves Simultaneous Multi-Sugar Fermentation in a Continuous Culture

Continuous culture fermentations were conducted to monitor sugar preferences and sugar consumption rates of CT2 and NKSW7-1 at different dilution rates. Due to specific growth rate differences between CT2 and NKSW7-1, we tested different dilution rates to optimize total sugar consumption and specific consumption rates without washing out biomass. Under a low dilution rate (0.13 h^{-1}) with a feeding medium containing 20 g/L of glucose, 20 g/L of mannose, 20 g/L of fructose, and 20 g/L of xylose, the CT2 strain consumed all hexose sugars (glucose, mannose, and fructose) (Figure 3A,C), while xylose was not consumed at all. At similar conditions (0.13 h^{-1}), the NKSW7-1 strain consumed all provided sugars at a rate of 0.039 g/g cell·h (Figure 3A,C) and maintained 8 g/L of each sugar in the bioreactor. An increase in dilution rate from 0.13 to 0.20 h^{-1} led to accumulation of 4.5 g/L glucose in the CT2-growing bioreactor, which in turn partially inhibited uptake of fructose and completely inhibited uptake of mannose and xylose (Figure 3B). CT2 was able to partially co-consume fructose while glucose accumulated (Figure 3D), which confirmed by our flask fermentation results (Figure 1B). As expected, NKSW7-1 was able to co-consume all sugars at similar rates regardless of dilution rate (Figure 3B,D). Despite kinetic inferiority to endogenous hexose transporters in yeast, AtSWEET7p expression could be advantageous for producing biofuels and chemicals from hexose and pentose mixtures due to alleviation of Crabtree effect glucose repression on uptake of other sugars.

2.7 | Transcriptomic and Metabolomic Analysis Shows Alleviated Glucose Repression in NKSW7-1

Our fermentation experiments demonstrated that NKSW7-1 can co-consume acetate in glucose presence (albeit at a slow rate) and hydrolyze sucrose rapidly under conditions with high glucose concentrations. We hypothesized that substitution of major hexose transporters by AtSWEET7p might have rewired the sugar metabolism and transcriptome of NKSW7-1. To understand the impact of *AtSWEET7* replacement of *HXT1-7* and *GAL2*, we performed transcriptomic and metabolomic analyses.

We first determined the minimum glucose concentration required for exerting the Crabtree effect in CT2, resulting in ethanol production even under high aeration conditions. CT2 with intact *HXT1-7* and *GAL2* produced 1.48 and 2.4 g/L of ethanol at glucose concentrations of 3 and 5 g/L, respectively (Supporting Information Figure 6A), and did not produce any

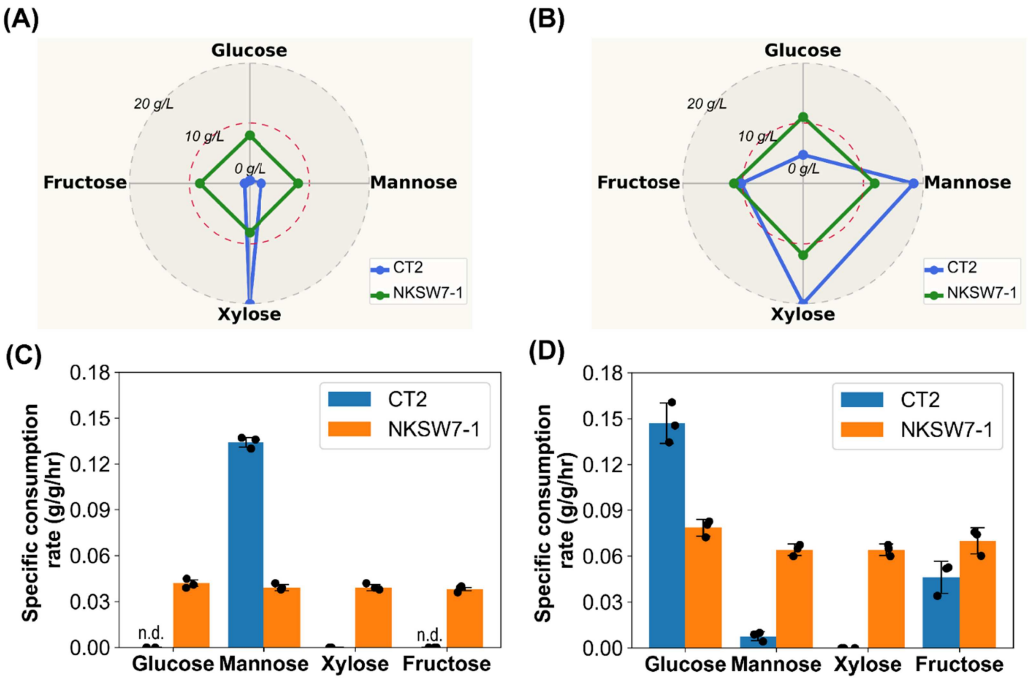

FIGURE 3 | Fermentation profile of CT2 and NKSW7-1 in continuous cultivation. Sugars remaining in bioreactors at dilution rate of (A) 0.13 h^{-1} and (B) 0.2 h^{-1}, respectively. Specific sugar consumption rates at dilution rate of (C) 0.13 h^{-1} and (D) 0.2 h^{-1}, respectively. Continuous culture was performed in bioreactors with 100 mL working volume at 30°C with 6 sL/h ambient air flow rate, 100 rpm stirring and pH control setup at 5.5. YP with 20 g/L of glucose, mannose, fructose, and xylose was continuously fed to bioreactor at specified dilution rates. Due to rapid consumption of glucose and fructose by CT2 at 0.13 h^{-1}, it was not possible to determine specific consumption rates of glucose and fructose by CT2. Therefore, they are reported as n.d. (not determined).

ethanol at 1 g/L of glucose. However, NKSW7-1 did not produce any ethanol under the same conditions (Supporting Information Figure 6B). We therefore chose to use 5 g/L of glucose as a basal condition for transcriptomic and metabolomic analysis.

We conducted RNA-seq experiments to measure gene expression differences between the parental CT2 and the *AtSWEET7*-integrated NKSW7-1 strains under 5 g/L of glucose. mRNA was isolated from biological triplicates of each strain during exponential growth (4 h). A total of 185,453,017 raw reads were obtained from the six total samples. Approximately 80%–85% of the reads were mapped into unique locations on the *S. cerevisiae* S288 reference genome (Supporting Information Figure 7). According to principal component analysis, CT2 and NKSW7-1 showed distinct expression patterns (Supporting Information Figure 8B). We applied a fold change of ≥ 1.5 and adjusted the *p*-value to a < 0.05 cutoff to subset genes with significantly different expression levels. In total, we identified 556 and 183 genes that were significantly up- and down-regulated, respectively, in NKSW7-1 as compared to CT2 (Supporting Information Figure 9). We excluded *HXT1-7* and *GAL2* from differential expression analysis due to complete substitution of those genes in NKSW7-1 by *AtSWEET7*. Details of the RNA-seq analysis are provided in Supporting Dataset S1.

To compare changes in metabolites between the CT2 and NKSW7-1 strains, we used gas chromatography-mass spectrometry (GC–MS). Principal component analysis showed distinct metabolome profiles between NKSW7-1 and CT2 (Supporting Information Figure 8A). Among the measured metabolites, 42 showed significant differences (significance cutoff for relative metabolite concentration > 2 and an adjusted *p*-value < 0.05) during growth in glucose between CT2 and NKSW7-1 (Supporting Information Figure 11). Detailed metabolome analysis results are provided in Supporting Dataset S2.

Remarkably, the majority of upregulated genes in NKSW7-1 are related to glucose repression and mitochondrion genes, such as *ICL1, IDP2, PCK1, JEN1, GAL1, CYB2, SUC2*, and so forth (Figure 4A, Supporting Information Figure 10) (Compagno et al. 2014; Kayikci and Nielsen 2015). Induction of *SUC2* was clearly demonstrated during the sugarcane juice and bagasse hydrolysate fermentation, where sucrose present in sugarcane juice was rapidly hydrolyzed by NKSW7-1 even in the presence of high glucose concentration (Figure 3). Not surprisingly, metabolomics analysis showed over-representation of TCA cycle-related metabolites, which correlates with transcriptome data (Figure 4A and Supporting Information Figure 11).

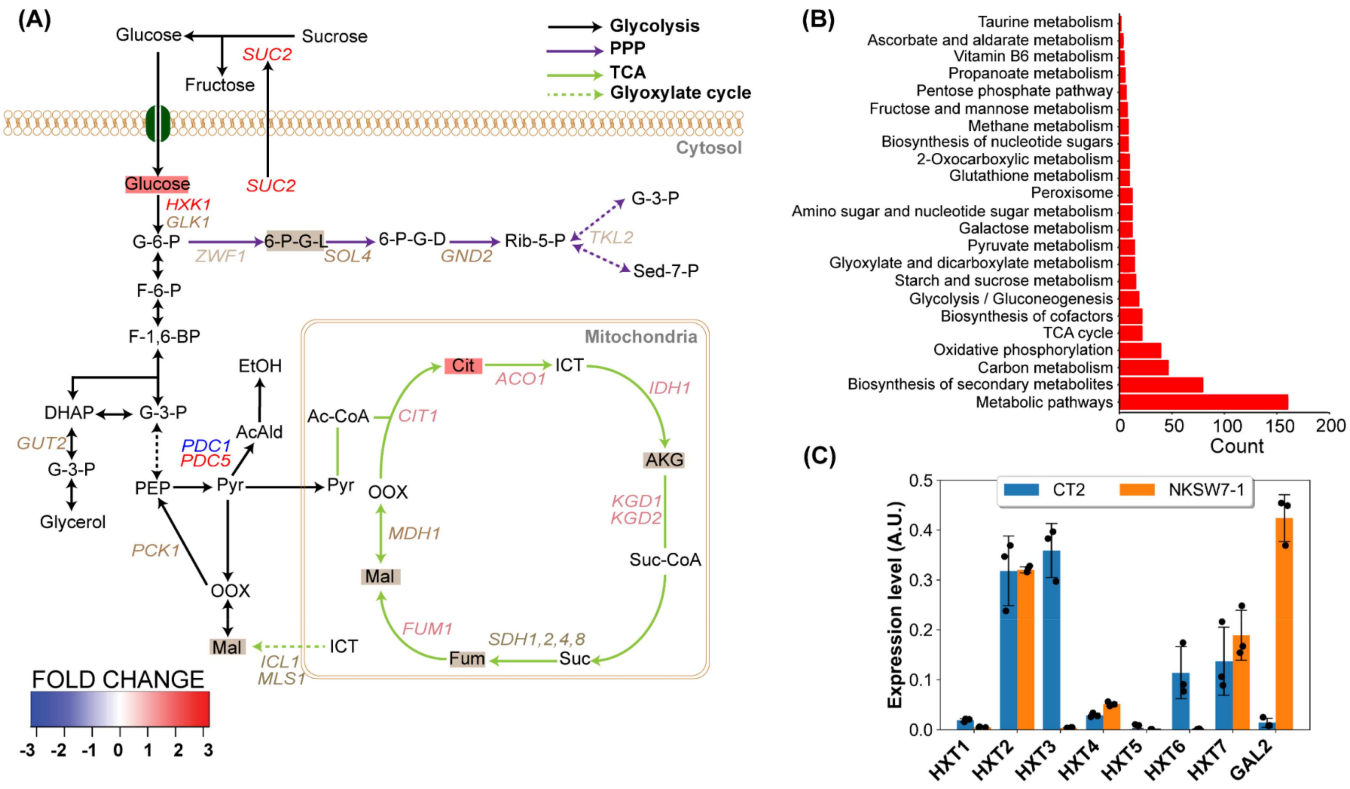

FIGURE 4 | Simplified summary of differentially expressed genes of NKSW7-1 grown in glucose. (A) Simplified central metabolic pathway of differentially expressed genes and metabolites in NKSW7-1. Significantly upregulated genes and metabolites are highlighted in color according to color key. For clarity, non-differentially expressed genes are omitted. Pathway enrichment analysis of differentially expressed genes in NKSW7-1 vs. CT2 using a cutoff *p*-value of 0.05. (B) Significantly upregulated pathway enrichment. (C) Expression level of native and *AtSWEET7* transporters in CT2 and NKSW7-1, respectively. Expression level measurements are based on reads mapped to the untranslated regions (UTRs) of the corresponding loci, which are identical for both CT2 and NKSW7-1. These reads reflect expression levels of native hexose transporters in CT2 and AtSWEET7 in NKSW7-1. 6-P-G-D, 6 phosphoglyconate; 6-P-G-L, 6 phosphogluconolactone; AcAld, acetaldehyde; Ac-CoA, acetyl-CoA; AKG, alphaketoglutarate; Cit, citrate; DHAP, dihydroxyacetone phosphate; EtOH, ethanol; Fum, fumarate; F-6-P, fructose 6 phosphate; GlyOx, glyoxylate; G-3-P, glycerol 3 phosphate; G-6-P, glucose 6 phosphate; ICT, isocitrate; Mal, malate; OOX, oxaloacetate; PEP, phosphoenolpyruvate; Pyr, pyruvate; Rib-5-P, ribulose 5 phosphate; Sed-7-P, sedoheptulose 7 phosphate; Suc-CoA, succinyl CoA; Suc, succinate; TCA, tricarboxylic acid cycle.

Next, we investigated the expression level of each of the *AtSWEET7* copies integrated into the *HXT1-7* and *GAL2* loci and compared it against the native transporters in CT2. Our results indicate that in the condition described above, CT2 upregulated *HXT2* and *HXT3* transporters, known to be high- and low-affinity glucose transporters, respectively (Özcan and Johnston 1999). *HXT2* transporter expression is known to be triggered at low glucose levels, while *HXT3* can be induced both at high and low glucose levels (Özcan and Johnston 1999). NKSW7-1 strains showed upregulation of *AtSWEET7* at *HXT2* and *GAL2* loci (Figure 4C). While *HXT2* locus-based overexpression was triggered by low glucose concentration, *GAL2* locus expression should be strongly inhibited by glucose presence, which is not the case for NKSW7-1 (Horak and Wolf 1997).

We further conducted pathway enrichment analysis to identify differential expression of pathways in NKSW7-1 in comparison to CT2. As expected, most identified upregulated genes are related to glucose repression and mitochondrial pathways, such as the TCA cycle, starch and sucrose metabolism, and oxidative phosphorylation (Figure 4B), while down-regulated genes are related to the biosynthesis of amino acids (Supporting Information Figures 12 and 13). Taken together, these results indicate that *AtSWEET7* integration broadly rewires yeast metabolism, triggering partial non-fermentable carbon and starvation signals even in the presence of glucose, explaining the abolishment of glucose repression on consumption of other sugars demonstrated above.

3 | Discussion

Numerous studies have attempted to address the co-fermentation problem of lignocellulosic sugars, with promising results (Hou et al. 2017; Nijland and Driessen. 2019). However, most were related to the engineering and/or bioprospecting of fungal sugar transporters classified under the Major Facilitator Superfamily. Most of these studies identified amino acid residues (such as Hxt11 N366 and Gal2 N376) in yeast hexose transporters in which mutations decrease glucose affinity, allowing xylose co-transport in *hxt* null background strains (Farwick et al. 2014; Nijland and Driessen. 2019; Shin et al. 2015). In contrast to this strategy, we instead replaced the native Hxt1-7p and Gal2p with AtSWEET7p originating from *A. thaliana*. The resulting NKSW7-1 strain demonstrated simultaneous co-transport of not only the major sugars in lignocellulosic biomass (glucose and xylose), but also other monosaccharides and sugar alcohol.

We posit that *AtSWEET7* is a highly promiscuous transporter with the capacity to transport a broad range of monosaccharides and sugar alcohols, as long as the host strain is able to metabolize them. As demonstrated, this broad transport capacity comes with a sacrifice in efficiency, with NKSW7-1 showing inferior sugar transport kinetics to the control strain CT2 with native hexose transporters (Supporting Information Figure 2) (Kuanyshev et al. 2021a). Though some may see this as a disadvantage, we believe *AtSWEET7* expression/integration in industrial hosts nonetheless would provide a unique opportunity to simultaneously convert diverse substrates into bioproducts in continuous fermentation conditions. Complete hydrolysis of lignocellulose yields glucose and xylose as major sugars and depending on lignocellulose origin additionally yields mannose and/or arabinose as minor sugars (Przybysz Buzała et al. 2017). However, most transporter studies have focused on glucose and xylose co-transport as a primary goal, omitting minor sugar co-transport (Hou et al. 2017; Nijland and Driessen. 2019). Recent studies demonstrated that overexpression of *Spathaspora passalidarum XUT1* transporter enabled simultaneous co-consumption of glucose and xylose in native xylose-consuming yeast *Ogatea polymorpha* and *Schefferomyces stipites*. However, authors did not use equal amounts of sugar to demonstrate true co-consumption, nor tested co-consumption of other hexose and/or sugar alcohols. In addition, glucose may compete with the xylose for binding to *SpXUT1* active site, hence affecting xylose or glucose transport rates. In the present study we demonstrate that AtSWEET7 is a broad range transporter that can support co-consumption of hexose and xylose. Consistent with this broad substrate permissiveness at the strain level, simultaneous utilization was observed in batch cultures with equal initial sugar concentrations (Long et al. 2012; Gao et al. 2023). For industrial-scale fermentations, the prospect of simultaneous bioconversion of such a wide range of substrates suggests increased economic feasibility of lignocellulosic biomass usage through application of *AtSWEET7*. The broad transport nature of AtSWEET7p could provide a platform to achieve total co-consumption of all sugars, and its inferior kinetics can still be addressed by protein engineering. As is, we have still demonstrated NKSW7-1 co-consumption of hexoses and pentoses under continuous culture conditions, a novel and exciting finding.

Continuous fermentation offers potential advantages over batch and fed-batch processes, including reduced operation costs, adaptation of industrial hosts to inhibitors either present in the substrate or accumulated as a product (ethanol, organic acids, etc.), and reduction in fermenter size (Brethauer and Wyman 2010). Importantly, continuous fermentation by nature requires co-consumption of all substrate components to avoid their accumulation, a condition that would exclude mixed-sugar fermentation of strains exhibiting glucose-repression. Attempts of hexose and pentose conversion in continuous culture conditions have historically been made using *Shefferomyces stipitis* and engineered *Zymomonas mobilis*. However, due to glucose preference, co-fermentation of sugars was nonetheless only possible in low glucose concentrations, which necessitates more sophisticated fermentation setups and increased operation costs (Grootjen et al. 1991; Krishnan et al. 2000; Lawford et al. 1998). Ha et al. demonstrated the applicability of continuous culture in co-fermenting glucose, cellobiose and xylose when xylose and cellobiose pathways were integrated into an industrial ethanol-producing *S. cerevisiae* strain (Ha et al. 2013). However, glucose was still consumed first, followed by co-fermentation of other sugars. Taken together, the previous studies have not yet demonstrated a complete solution to co-consumption of sugar mixtures in continuous culture conditions. As shown from our continuous cultures (Figure 3), NKSW7-1 is an "all you can eat" strain able to metabolize a mixture of four different sugars at equal rates, regardless of dilution rate, while the CT2 control strain showed accumulation of non-glucose sugars due to the glucose preference of native Hxt1-7p and Gal2p transporters (Figure 3). Among the currently studied solutions to glucose

repression in *S. cerevisiae*, we believe AtSWEET7p to hold the greatest potential in enabling industrially relevant levels of sugar co-consumption.

Glucose repression in *S. cerevisiae* consists of fine-tuned control of both hexose transporter expression and internal metabolism, enabling rapid overflow metabolism of glucose and ethanol production even in the presence of oxygen in a phenomenon known as the Crabtree effect (Compagno et al. 2014; Hagman et al. 2014; Kayikci and Nielsen 2015). In *S. cerevisiae*, the Crabtree effect takes effect in glucose concentrations as low as 3 g/L (Supporting Information Figure 6A).

As such, native hexose transporters have a high affinity toward glucose, meaning during mixed sugar fermentation *S. cerevisiae* ferments glucose before other sugars (Subtil and Boles 2012) (Figures 1 and 2). In this study, we have uncovered the extensive transcriptomic and metabolomic rewiring of sugar metabolism in *S. cerevisiae* induced by AtSWEET7p substitution of major hexose transporters (Özcan et al. 1997; Persson et al. 2020). Our transcriptomic analysis clearly demonstrated that NKSW7-1 upregulated the majority of glucose-repressed genes related to alternative carbon utilization, respiration, and the TCA cycle (Figure 4A). We hypothesize that replacement of native transporters by the kinetically inferior AtSWEET7p led to a decrease in the energy state of cells due to slower glucose uptake and metabolism.

In *S. cerevisiae*, the switch between fermentation of glucose to respiration and alternative carbon source use is orchestrated by several transcriptional factors. Among them, Snf1 plays a key role by regulating repressors and activators (Compagno et al. 2014; García-Salcedo et al. 2014; Hagman et al. 2014; Kayikci and Nielsen 2015). We believe in NKSW7-1 slow glucose uptake mediated by kinetically slow AtSWEET7 triggers Snf1 activation, which in turn phosphorylates Hxk2 and Mig1, activating a cascade of glucose-repressed genes, as supported by our transcriptomic data (Figure 4) (Fernández-García et al. 2012; Nonaka et al. 2025). In addition, our metabolomics data showed an 8.6-fold increase in intracellular glucose concentration in NKSW7-1 in comparison to CT2 (Supporting Information Figure 11, Supporting Dataset S2). This suggests decreased hexokinase activity and slower glycolysis due to Snf1 activation secondary to slower uptake of glucose by AtSWEET7p. Increase in TCA metabolites and reduction of PDC1 transcript level strongly supports low glucose-triggered metabolic shift and strong activation of glucose-repressed genes, such as *SUC2*, *PDC5*, and *GAL2* (Figure 4).

Remarkably, during sugarcane juice and bagasse hydrolysate fermentation, NKSW7-1 also rapidly hydrolyzed sucrose into glucose and fructose, which were then co-fermented together with the remaining xylose and glucose (Figure 2). This hydrolysis, a result of the *SUC2* gene product (invertase) is another target of the glucose repression that is alleviated in NKSW7-1 (Özcan et al. 1997; Persson et al. 2020). This occurrence may be advantageous for industrial feedstock processes where invertase activity is desired.

AtSWEET7p expression has the potential to simultaneously convert various sugars and sugar mixtures into valuable products. The extreme promiscuity of AtSWEET7p in co-transporting myriad monosaccharides and a sugar alcohol as demonstrated here would allow its use in various applications where sugar mixtures are concerned, including industrially relevant and underutilized substrates such as lignocellulosic biomass. In addition, AtSWEET7p holds value not only in monosaccharide transport but also as an exporter due to its ability for bidirectional transportation. For example, AtSWEET7p's capacity to co-transport glucose/xylose and export xylitol could be utilized in industrial xylitol production (Chen 2014; Xue et al. 2022). In this study, Xyl2p which is responsible for conversion of xylitol into xylulose, was deleted in both CT2 and NKSW7-1. NKSW7-1 efficiently fermented both glucose and xylose simultaneously and produced xylitol with a yield of 0.93 g xylitol/g xylose (Figure 5B), while CT2 started slow production of xylitol only after glucose was depleted (Figure 5A).

Sole xylose metabolism leads to diminished Crabtree effect channeling pyruvate to both TCA and PDH bypass routes. Recent study demonstrated that when xylose used as sole carbon source, redirecting pyruvate into only PDH bypass significantly improves 3-HP titers (Li et al. 2025). In this context, when mixture of glucose and xylose is used, NKSW7-1 still capable to induce partial Crabtree effect at glucose concentrations above 5 g/L, so pyruvate could be channeled to PDH bypass. This property of multi-sugar consumption of NKSW7-1

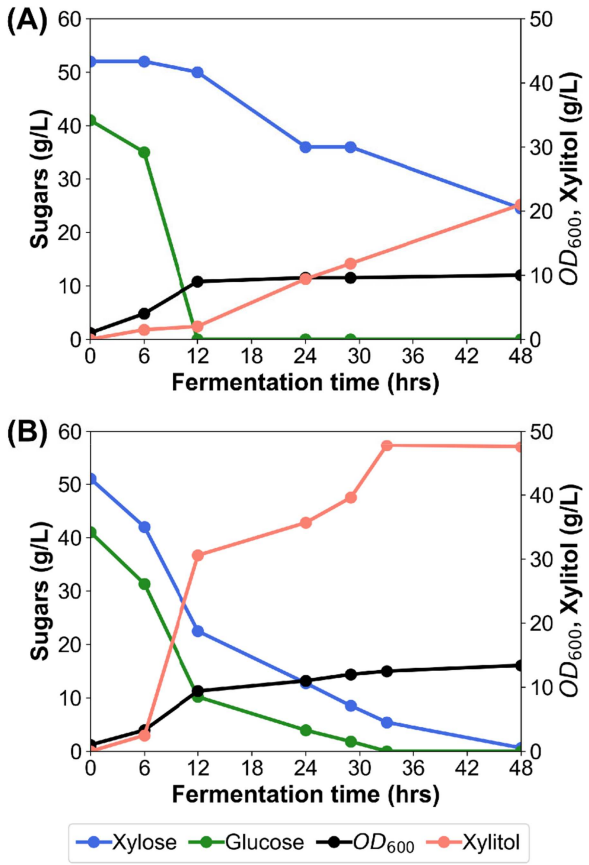

FIGURE 5 | Xylitol production profile of Xyl2Δ CT2 and NKSW7-1 strains. Fermentation profile of (A) CT2 Xyl2Δ and (B) NKSW7-1 Xyl2Δ. Cells were precultured in YP with glucose and inoculated into YP with glucose and xylose at 50 and 40 g/L, respectively, at OD600 1. Cells were incubated at 100 rpm and 30°C. Values are the means of two independent experiments, and error bars indicate standard error.

can be beneficial for bio-based production of pyruvate-derived chemicals.

Finally, it is worth mentioning that the *AtSWEET7* used here is of a native variant, which opens the door for future studies to improve kinetics and enable selectivity (if necessary) by means of rational and directed evolution. We envision a future where AtSWEET7p phenotypes can be tuned through rational design to optimize for a variety of industrial hosts and applications.

4 | Materials and Methods

4.1 | Strains and Media

E. coli Top10 [F-*mcr*A Δ(*mrr-hsd*RMS-*mcr*BC) φ80*lac*ZΔM15 Δ*lac*X74 *rec*A1 *ara*D139 Δ(*ara-leu*) 7697 *gal*U *gal*K *rps*L (Str^R) *end*A1 *nup*G] was used for manipulation of plasmids. The *E. coli* strains were grown in Luria-Bertani (LB) medium (1% tryptone, 0.5% yeast extract, 1% NaCl) at 37°C with ampicillin (100 μg/mL) as necessary. The CT2 strain, and its derived yeast strains were cultivated at 30°C in YP medium (10 g/L yeast extract, 20 g/L peptone) with 20 g/L of glucose. For CRISPR-Cas9 based genome editing experiments, 120 μg/mL of nourseothricin was added as necessary for selecting transformants.

4.2 | Strain and Plasmid Construction

A xylose-fermenting *S. cerevisiae* CT2 strain—a D452-2 derived strain with integration of two copies of expression cassettes containing *XYL1*, *XYL2*, and *XYL3* in the background of *PHO13* and *ALD6* deletion (Tsai et al. 2015)—was used as a host strain for replacing major hexose transporters with *AtSWEET7*. The oligonucleotides and synthetic genes used in this study are listed in Supporting Information Table 1. Yeast transformations were performed using a previously described lithium acetate method (Gietz and Schiestl 2007). A Cas9 system developed previously in our lab was used for targeted integration of *AtSWEET7* and deletion of *XYL2* (Kuanyshev et al. 2021b). This gRNA cloning into a Cas9 and gRNA expressing plasmid (pCast) is briefly described as follows: First, pCast plasmid was linearized with *Aar*I enzyme and gel purified (Thermo Fisher Scientific, USA). Second, 20 bp oligonucleotides with appropriate sticky end overhangs were self-annealed to yield duplex DNA, which was ligated to pCast using T4 DNA ligase according to manufacturer protocol (New England Biolabs, USA). CHOPCHOP (version 3) gRNA design web tool was used for *S. cerevisiae* gRNA design (Labun et al. 2019). *S. cerevisiae* codon optimized *AtSWEET7* was synthesized by Twist Bioscience (San Francisco, CA). For targeted integration of *AtSWEET7* into *HXT1-7* and *GAL2* loci, donor *AtSWEET7* with 40 bp homology arms was amplified in PCR using Q5 high-fidelity polymerase (New England Biolabs, USA). Donor and pCast plasmid targeting *HXT1-7 or GAL2* were co-transformed according to the lithium acetate-based protocol mentioned above. Cells were selected on yeast extract-peptone (YP) plate (10 g/L yeast extract, 20 g/L peptone) containing glucose (YPD) supplemented with 120 μg/mL nourseothricin (Gold Biotechnology, USA). To construct the Xyl2 deletion strain, gRNA targeting *XYL2* was also constructed as described above.

4.3 | Sugarcane Juice Extraction

Processing of sugarcane was conducted at a translational research facility, the Integrated Bioprocessing Research Laboratory, located at the University of Illinois at Urbana–Champaign, Urbana, IL. Fresh sugarcane was squeezed using a pilot-scale juice extractor. Approximately 190 kg of harvested sugarcane was squeezed twice, the juice from which was collected and stored at 4°C. The crushed stem was processed through a fiber press to recover residual juice. The leftover bagasse was stored at 4°C.

4.4 | Bagasse Pretreatment and Hydrolysis

The bagasse was washed to remove adhering free sugars and dried to meet the desired moisture content (50%) for hydrothermal pretreatment in a continuous hydrothermal reactor. The pretreatment was performed at 190°C for 10 min. After the pretreatment, the biomass was dried at 40°C in a tray dryer (The National Drying Machinery Co., USA) to a moisture content of 15%. The dried pretreated bagasse was disc milled using an electrical power burr mill (Meadows Mills Inc., USA). The disc mill consists of closely spaced stationary and rotating disks (6 in. in diameter). The distance between the two disks was set at the minimum allowable gap (Cheng et al. 2019; Cheng et al. 2020).

Fed-batch enzymatic hydrolysis was performed at 50°C for 72 h with 30% (w/v) solids in an 80 L reactor. Enzymatic hydrolysis started at 20% solids, and the remaining biomass was added after 3 h. Furthermore, the surfactant PEG 4000 was added at 2% based on the total biomass load to facilitate mass transport. Cellulase and hemicellulase cocktails and deionized water were added to achieve the target solids load. NS 22257 (Novozymes North America Inc., USA) was added at 50 FPU/g biomass (15 mg cellulase protein/g dry substrate) and NS22244 (Novozymes North America Inc., USA) at 3.75 mg hemicellulase protein/g dry biomass were added at the beginning of the reaction to achieve the final solid content of 30% w/v. The hydrolysate was separated and sterilized by filtration using 0.22 μm pore size cellulose nitrate membrane (Cheng et al. 2020).

4.5 | Flask Fermentation Experiments

For all flask fermentations, yeast cells were precultured in YPD20 (YP medium with 20 g/L of glucose) at 30°C and 250 rpm, unless otherwise specified. Yeast precultures were grown overnight in YPD medium in 5 mL tubes and harvested at mid-exponential phase. Cells were then washed twice with sterilized water and inoculated at appropriate cell density into 125-mL Erlenmeyer flasks with 25 mL YP medium with added sugars. For bagasse hydrolysate (BH) and sugarcane juice (SCJ) fermentations, cells were additionally transferred and precultured in 25 mL of YP media + 25% bagasse hydrolysate with pH adjusted to 5.5 with KOH to adapt cells for inhibitors. Grown cells were harvested at mid-exponential phase and inoculated into 25 mL of either YP + 25% BH or YP + 25% BH + 50% SCJ at $OD_{600} = 1$, unless otherwise specified. All fermentations were held at 30°C and at 100 rpm in a MaxQ 4000 orbital shaker (Thermo Fisher Scientific Inc., USA) unless

otherwise specified. All experiments were repeated independently in duplicate with variation indicated in figures with error bars. BH and SCJ composition is summarized in Supporting Information Table 2.

4.6 | Continuous Culture Fermentation

Continuous culture fermentation was conducted in 250 mL Eppendorf DASbox Mini Bioreactors (Eppendorf, Germany) with working volume of 100 mL. Bioreactors were set to maintain a pH of 5.5, agitation of 100 rpm, temperature of 30°C, and air flow rate of 6 standard liters per minute. Antifoam 204 was added to control foaming as necessary (typically 1 drop per reactor). YP medium with 20 g/L of glucose, mannose, fructose, and xylose was supplied continuously, and the same amount of culture volume was removed using Masterflex L/S peristaltic pumps (Cole–Parmer, USA), sustaining total culture volume. For CT2, continuous culture was operated at dilution rates ranging from 0.13 to 0.38 h^{-1} and for NKSW7-1 from 0.13 to 0.23 h^{-1}. The steady state of the continuous culture was determined by stably maintaining biomass and sugar concentrations after a period of at least 2 residence times (1/D) at each dilution rate condition. Continuous culture parameters and results were calculated by the following mass balance methods described by Kang et al. (Kang et al. 2022).

4.7 | Dry Cell Weight and Cell Density Measurements

Cell density was monitored by optical density (OD) at 600 nm using Biomate 3 UV-visible spectrophotometer (Thermo Fisher Scientific Inc., USA). Dry weight calculations were performed by harvesting 2 × 5 mL samples in pre-weighed, desiccated sample vials, and the cell pellet recovered by centrifugation at 5000 × g for 5 min, at 4°C. The cells were subsequently washed twice with 5 mL ice-cold ultrapure water, and recovered by centrifugation, as above. The pellets were then dried for 24 h at 110°C and stored in a desiccator prior to being weighed.

4.8 | Analytical Methods

Fermentation metabolite concentrations were analyzed by a 1200 series high-performance liquid chromatography (Agilent Technologies Inc., USA) instrument equipped with refractive index detector using a Rezex ROA-Organic Acid H^+ (8%) column (Phenomenex Inc., USA) for ethanol, xylitol, and glycerol measurements and Rezex RCM-Monosaccharide Ca^- column (Phenomenex Inc., USA) for hexose and pentose measurements. The column was eluted with 0.005 N of H_2SO_4 at a flow rate of 0.6 mL/min at 50°C or ultrapure water at a flow rate of 0.6 mL/min at 80°C. pH was monitored using a PHM210 pH meter (Radiometer Analytical SAS, France) with attached Accumet 13-620-290 pH probe (Thermo Fisher Scientific Inc., USA).

4.9 | Transcriptomics Analysis

To analyze the gene expression profiles of CT2 and NKSW7-1, RNA samples were extracted from YPD5 (YP medium with 5 g/L of glucose) cultures grown at 30°C and 250 rpm, after 4 h growth. Total RNA was extracted using a Quick-RNA Fungal/Bacterial Kits (Zymo Research, USA) and then treated with DNA-free DNase using the TURBO DNA-free kit (Thermo Fisher Scientific, Waltham, MA) to remove genomic DNA. RNA sequencing was performed at the Roy J. Carver Biotechnology Center at the University of Illinois at Urbana–Champaign, IL. Raw and processed RNA-seq files were uploaded to NCBI (NCBI Accession number: GSE238127).

Adapters and low-quality reads were trimmed using Trimmomatic (Bolger et al. 2014). Trimmed reads were mapped onto *S. cerevisiae* S288C reference genome (RefSeq assembly accession: GCF_000146045.2) using STAR version 2.6.1b (Dobin et al. 2013). Read counts for each gene were calculated using featureCounts from the Subread package, version 1.5.2 (Liao et al. 2014). Differential expression analysis was performed in R using edgeR and limma (Ritchie et al. 2015; Robinson et al. 2010). Glimma and gplots were used for graphical representation of expression data (Su et al. 2017). Functional annotations were obtained from the Saccharomyces Genome Database (SGD) (Cherry et al. 2012). Pathway enrichment with differential expression data was performed using ShinyGO (Ge et al. 2020).

4.10 | Analysis of Metabolites by Using GC–MS

To extract intracellular metabolites from yeast, cells were cultivated in YPD5 (YP medium with 5 g/L of glucose) at 30°C and 250 rpm. One milliliter of OD 5 cell culture was harvested at 4 h and centrifuged at 15,000 rpm for 1 min. To wash the cells, 1 mL of distilled water was added and after vigorous vortexing the mixture was centrifuged at 15,000 rpm for 1 min, which was repeated twice. To extract the intracellular metabolites, cell pellets were resuspended to 1 mL of pure methanol −20°C, sonicated −20°C for 5 min using a VWR Ultrasonic Cleaner (VWR, USA), and vortexed for 5 min. After centrifugation at 16,100 × g for 5 min at 4°C, 800 μL of supernatant was transferred to a new 1.7 mL microcentrifuge tube and dried under reduced pressure in a Savant SPD1010 Speed-Vac Scientific, USA) until all solvents evaporated.

To identify and quantify metabolites using GC/MS, methoximation and silylation were performed. For methoximation, 20 μL of 40 mg/mL methoxyamine hydrochloride (226904, Sigma-Aldrich, USA) in pyridine (360570, Sigma-Aldrich, USA) was added to the tubes containing metabolites, and the mixture was incubated at 30°C for 90 min. For silylation, 50 μL of N-methyl-N-trimethylsilyl-trifluoroacetamide (69479, Sigma-Aldrich, USA) was added to the mixture, which was incubated at 37°C for 30 min.

An Agilent 7890 A GC coupled with a quadrupole MS5975C system (Agilent Technologies, USA) was used for analysis of metabolites. A 1.0 μL aliquot of the derivatized sample was injected into the GC, in splitless mode. The metabolites were separated on an RTX-5Sil MS column (30 m length, 0.25 mm inner diameter, and 0.25 μm film thickness, Restek) with an additional 10 m guard column. The initial oven temperature was set at 50°C for 1 min and was then ramped to 330°C at a rate of 20°C/min then held at 330°C for 5 min. Mass spectra were recorded over a mass range of 85–550 m/z. The

temperatures of the ion source and transfer line of the MS were set at 250°C and 280°C, respectively. The sample was ionized by electron impact at 70 eV. For the processing of GC/MS data, MS dial (version 4.24) was used. The latest All records with Fiehn RI Library provided by MS-DIAL were used to identify metabolites by matching the mass spectra of peaks. Since the retention index marker was not used, the retention time tolerance was set to 1 min. Metabolites that showed significant differences between the boiling temperature of the metabolite and the oven temperature at the signal retention time were removed from the data. Except for the retention time setting, the default settings were used. For statistical analysis of metabolome data, MetaboAnalyst (https://www.metaboanalyst.ca/; version 5.0) was used.

Author Contributions

Nurzhan Kuanyshev: writing – review and editing, writing – original draft, methodology, investigation, formal analysis, data curation, visualization, conceptualization. **Degaulle Dai:** writing – review and editing, investigation, visualization. **Jungyeon Kim:** investigation, formal analysis, data curation, visualization. **Nam Kyu Kang:** investigation, methodology. **Ming-Hsun Cheng:** methodology, resources. **Vijay Singh:** methodology, resources. **Yong-Su Jin:** writing – review and editing, methodology, data curation, conceptualization, funding acquisition, resources, supervision.

Acknowledgments

This work was funded by the DOE Center for Advanced Bioenergy and Bioproducts Innovation (U.S. Department of Energy, Office of Science, Office of Biological and Environmental Research under Award Number DE-SC0018420). Any opinions, findings, and conclusions or recommendations expressed in this publication are those of the author(s) and do not necessarily reflect the views of the U.S. Department of Energy.

Conflicts of Interest

The authors declare no conflicts of interest.

References

Bokinsky, G., P. P. Peralta-Yahya, A. George, et al. 2011. "Synthesis of Three Advanced Biofuels From Ionic Liquid-Pretreated Switchgrass Using Engineered *Escherichia Coli*." *Proceedings of the National Academy of Sciences* 108: 19949–19954.

Bolger, A. M., M. Lohse, and B. Usadel. 2014. "Trimmomatic: A Flexible Trimmer for Illumina Sequence Data." *Bioinformatics* 30: 2114–2120.

Brethauer, S., and C. E. Wyman. 2010. "Review: Continuous Hydrolysis and Fermentation for Cellulosic Ethanol Production." *Bioresource Technology* 101: 4862–4874.

Carroll, A., and C. Somerville. 2009. "Cellulosic Biofuels." *Annual Review of Plant Biology* 60: 165–182.

Chen, L. Q. 2014. "Sweet Sugar Transporters for Phloem Transport and Pathogen Nutrition." *New Phytologist* 201: 1150–1155.

Cheng, M. H., B. S. Dien, D. K. Lee, and V. Singh. 2019. "Sugar Production From Bioenergy Sorghum by Using Pilot Scale Continuous Hydrothermal Pretreatment Combined With Disk Refining." *Bioresource Technology* 289: 121663.

Cheng, M. H., H. J. Kadhum, G. S. Murthy, B. S. Dien, and V. Singh. 2020. "High Solids Loading Biorefinery for the Production of Cellulosic Sugars From Bioenergy Sorghum." *Bioresource Technology* 318: 124051.

Cherry, J. M., E. L. Hong, C. Amundsen, et al. 2012. "Saccharomyces Genome Database: The Genomics Resource of Budding Yeast." *Nucleic Acids Research* 40: D700–D705.

Clomburg, J. M., A. M. Crumbley, and R. Gonzalez. 2017. "Industrial Biomanufacturing: The Future of Chemical Production." *Science* 355, no. 6320: aag0804-38.

Compagno, C., S. Dashko, and J. Piškur. 2014. "Introduction to Carbon Metabolism in Yeast." In *Molecular Mechanisms in Yeast Carbon Metabolism*, edited by J. Piškur and C. Compagno, 1–19. Springer Berlin Heidelberg.

Cysewski, G. R., and C. R. Wilke. 1978. "Process Design and Economic Studies of Alternative Fermentation Methods for the Production of Ethanol." *Biotechnology and Bioengineering* 20: 1421–1444.

Dobin, A., C. A. Davis, F. Schlesinger, J. Drenkow, C. Zaleski, and S. Jha. 2013. "Star: Ultrafast Universal RNA-Seq Aligner." *Bioinformatics* 29: 15–21.

Farwick, A., S. Bruder, V. Schadeweg, M. Oreb, and E. Boles. 2014. "Engineering of Yeast Hexose Transporters to Transport D-Xylose Without Inhibition by D-Glucose." *Proceedings of the National Academy of Sciences* 111: 5159–5164.

Fernández-García, P., R. Peláez, P. Herrero, and F. Moreno. 2012. "Phosphorylation of Yeast Hexokinase 2 Regulates Its Nucleocytoplasmic Shuttling." *Journal of Biological Chemistry* 287: 42151–42164.

Gao, M., Y. Zhao, Z. Yao, Q. Su, P. Van Beek, and Z. Shao. 2023. "Xylose and Shikimate Transporters Facilitates Microbial Consortium as a Chassis for Benzylisoquinoline Alkaloid Production." *Nature Communications* 14: 7797. https://doi.org/10.1038/s41467-023-43049-w.

García-Salcedo, R., T. Lubitz, G. Beltran, et al. 2014. "Glucose De-Repression by Yeast AMP-Activated Protein Kinase Snf1 Is Controlled Via at Least Two Independent Steps." *FEBS Journal* 281: 1901–1917.

Gárdonyi, M., M. Jeppsson, G. Lidén, M. F. Gorwa-Grauslund, and B. Hahn-Hägerdal. 2003. "Control of Xylose Consumption by Xylose Transport in Recombinant *Saccharomyces cerevisiae*." *Biotechnology and Bioengineering* 82: 818–824.

Ge, S. X., D. Jung, and R. Yao. 2020. "Shinygo: A Graphical Gene-Set Enrichment Tool for Animals and Plants." *Bioinformatics* 36: 2628–2629.

Gietz, R. D., and R. H. Schiestl. 2007. "High-Efficiency Yeast Transformation Using the LiAc/SS Carrier DNA/PEG Method." *Nature Protocols* 2: 31–34.

Grootjen, D. R. J., M. L. Jansen, R. G. J. M. van der Lans, and K. C. A. M. Luyben. 1991. "Reactors in Series for the Complete Conversion of Glucose/Xylose Mixtures by *Pichia stipitis* and *Saccharomyces cerevisiae*." *Enzyme and Microbial Technology* 13: 828–833.

Ha, S. J., S. R. Kim, H. Kim, J. Du, J. H. D. Cate, and Y. S. Jin. 2013. "Continuous Co-Fermentation of Cellobiose and Xylose by Engineered *Saccharomyces cerevisiae*." *Bioresource Technology* 149: 525–531.

Hagman, A., T. Säll, and J. Piškur. 2014. "Analysis of the Yeast Short-Term Crabtree Effect and Its Origin." *FEBS Journal* 281: 4805–4814.

Hamacher, T., J. Becker, M. Gárdonyi, B. Hahn-Hägerdal, and E. Boles. 2002. "Characterization of the Xylose-Transporting Properties of Yeast Hexose Transporters and Their Influence on Xylose Utilization." *Microbiology* 148: 2783–2788.

Horak, J., and D. H. Wolf. 1997. "Catabolite Inactivation of the Galactose Transporter in the Yeast *Saccharomyces cerevisiae*: Ubiquitination, Endocytosis, and Degradation in the Vacuole." *Journal of Bacteriology* 179: 1541–1549.

Hou, J., C. Qiu, Y. Shen, H. Li, and X. Bao. 2017. "Engineering of *Saccharomyces cerevisiae* for the Efficient Co-Utilization of Glucose and Xylose." *FEMS Yeast Research* 17: fox034.

Jeena, G. S., S. Kumar, and R. K. Shukla. 2019. "Structure, Evolution and Diverse Physiological Roles of Sweet Sugar Transporters in Plants." *Plant Molecular Biology* 100: 351–365.

Jeffries, T. W., and Y. S. Jin. 2004. "Metabolic Engineering for Improved Fermentation of Pentoses by Yeasts." *Applied Microbiology and Biotechnology* 63: 495–509.

Jin, Y. S., H. Ni, J. M. Laplaza, and T. W. Jeffries. 2003. "Optimal Growth and Ethanol Production From Xylose by Recombinant *Saccharomyces cerevisiae* Require Moderate D-Xylulokinase Activity." *Applied and Environmental Microbiology* 69: 495–503.

Jönsson, L. J., B. Alriksson, and N. O. Nilvebrant. 2013. "Bioconversion of Lignocellulose: Inhibitors and Detoxification." *Biotechnology for Biofuels* 6: 16.

Jordan, P., J. Y. Choe, E. Boles, and M. Oreb. 2016. "Hxt13, Hxt15, Hxt16, and Hxt17 From *Saccharomyces cerevisiae* Represent a Novel Type of Polyol Transporters." *Scientific Reports* 6: 23502.

Kang, N. K., M. Kim, K. Baek, Y. K. Chang, D. R. Ort, and Y.-S. Jin. 2022. "Photoautotrophic Organic Acid Production: Glycolic Acid Production by Microalgal Cultivation." *Chemical Engineering Journal* 433: 133636.

Kayikci, Ö., and J. Nielsen. 2015. "Glucose Repression in *Saccharomyces cerevisiae*." *FEMS Yeast Research* 15: fov068.

Kim, S. R., S. J. Ha, N. Wei, E. J. Oh, and Y. S. Jin. 2012. "Simultaneous Co-Fermentation of Mixed Sugars: A Promising Strategy for Producing Cellulosic Ethanol." *Trends in Biotechnology* 30: 274–282.

Kim, S. R., J. M. Skerker, W. Kang, et al. 2013. "Rational and Evolutionary Engineering Approaches Uncover a Small Set of Genetic Changes Efficient for Rapid Xylose Fermentation in *Saccharomyces cerevisiae*." *PLoS One* 8: e57048.

Krishnan, M. S., M. Blanco, C. K. Shattuck, N. P. Nghiem, and B. H. Davison. 2000. "Ethanol Production From Glucose and Xylose by Immobilized *Zymomonas mobilis* CP4 (pZB5)." *Applied Biochemistry and Biotechnology* 84–86: 525–542.

Kuanyshev, N., A. Deewan, S. S. Jagtap, et al. 2021a. "Identification and Analysis of Sugar Transporters Capable of Co-Transporting Glucose and Xylose Simultaneously." *Biotechnology Journal* 16: e2100238.

Kuanyshev, N., C. V. Rao, B. Dien, and Y. S. Jin. 2021b. "Domesticating a Food Spoilage Yeast Into an Organic Acid-Tolerant Metabolic Engineering Host: Lactic Acid Production by Engineered *Zygosaccharomyces bailii*." *Biotechnology and Bioengineering* 118: 372–382.

Labun, K., T. G. Montague, M. Krause, Y. N. Torres Cleuren, H. Tjeldnes, and E. Valen. 2019. "Chopchop v3: Expanding the Crispr Web Toolbox Beyond Genome Editing." *Nucleic Acids Research* 47: W171–W174.

Lawford, H. G., J. D. Rousseau, A. Mohagheghi, and J. D. McMillan. 1998. "Continuous Culture Studies of Xylose-Fermenting *Zymomonas mobilis*." *Applied Biochemistry and Biotechnology* 70–72: 353–367.

Lee, J. W., S. Yook, H. Koh, C. V. Rao, and Y. S. Jin. 2021. "Engineering Xylose Metabolism in Yeasts to Produce Biofuels and Chemicals." *Current Opinion in Biotechnology* 67: 15–25.

Li, H., O. Schmitz, and H. S. Alper. 2016. "Enabling Glucose/Xylose Co-Transport in Yeast Through the Directed Evolution of a Sugar Transporter." *Applied Microbiology and Biotechnology* 100: 10215–10223.

Li, X., Y. Wang, X. Chen, et al. 2025. "Modular Deregulation of Central Carbon Metabolism for Efficient Xylose Utilization in *Saccharomyces cerevisiae*." *Nature Communications* 16: 4551. https://doi.org/10.1038/s41467-025-59966-x.

Liao, Y., G. K. Smyth, and W. Shi. 2014. "Featurecounts: An Efficient General Purpose Program for Assigning Sequence Reads to Genomic Features." *Bioinformatics* 30: 923–930.

Long, T. M., Y.-K. Su, J. Headman, A. Higbee, L. B. Willis, and T. W. Jeffries. 2012. "Cofermentation of Glucose, Xylose, and Cellobiose by the Beetle-Associated Yeast *Spathaspora passalidarum*." *Applied and Environmental Microbiology* 78: 5492–5500. https://doi.org/10.1128/AEM.00374-12.

Nijland, J. G., and A. J. M. Driessen. 2020. "Engineering of Pentose Transport in *Saccharomyces cerevisiae* for Biotechnological Applications." *Frontiers in Bioengineering and Biotechnology* 7: 464.

Nonaka, K., K. Nishimura, K. Uesaka, et al. 2025. "Snf1 and Yeast GSK3-β Activate Tda1 to Suppress Glucose Starvation Signaling." *EMBO Reports* 26: 2910–2930.

Özcan, S., L. G. Vallier, J. S. Flick, M. Carlson, and M. Johnston. 1997. "Expression of the *SUC2* Gene of *Saccharomyces cerevisiae* Is Induced by Low Levels of Glucose." *Yeast* 13: 127–137.

Özcan, S., and M. Johnston. 1999. "Function and Regulation of Yeast Hexose Transporters." *Microbiology and Molecular Biology Reviews* 63: 554–569.

Palmqvist, E., and B. Hahn-Hägerdal. 2000. "Fermentation of Lignocellulosic Hydrolysates. II: Inhibitors and Mechanisms of Inhibition." *Bioresource Technology* 74: 25–33.

Parachin, N. S., B. Bergdahl, E. W. J. van Niel, and M. F. Gorwa-Grauslund. 2011. "Kinetic Modelling Reveals Current Limitations in the Production of Ethanol From Xylose by Recombinant *Saccharomyces cerevisiae*." *Metabolic Engineering* 13: 508–517.

Persson, S., N. Welkenhuysen, S. Shashkova, and M. Cvijovic. 2020. "Fine-Tuning of Energy Levels Regulates SUC2 via a Snf1-Dependent Feedback Loop." *Frontiers in Physiology* 11: 954.

Podolsky, I. A., S. Seppala, H. Xu, Y. S. Jin, and M. A. O'Malley. 2021. "A SWEET Surprise: Anaerobic Fungal Sugar Transporters and Chimeras Enhance Sugar Uptake in Yeast." *Metabolic Engineering* 66: 137–147.

Przybysz Buzała, K., H. Kalinowska, P. Przybysz, and E. Małachowska. 2017. "Conversion of Various Types of Lignocellulosic Biomass to Fermentable Sugars Using Kraft Pulping and Enzymatic Hydrolysis." *Wood Science and Technology* 51: 873–885.

Reider Apel, A., M. Ouellet, H. Szmidt-Middleton, J. D. Keasling, and A. Mukhopadhyay. 2016. "Evolved Hexose Transporter Enhances Xylose Uptake and Glucose/Xylose Co-Utilization in *Saccharomyces cerevisiae*." *Scientific Reports* 6: 19512.

Ritchie, M. E., B. Phipson, D. Wu, et al. 2015. "Limma Powers Differential Expression Analyses for RNA-Sequencing and Microarray Studies." *Nucleic Acids Research* 43: e47.

Robertson, G. P., S. K. Hamilton, B. L. Barham, et al. 2017. "Cellulosic Biofuel Contributions to a Sustainable Energy Future: Choices and Outcomes." *Science* 356, no. 6345: eaal2324.

Robinson, M. D., D. J. McCarthy, and G. K. Smyth. 2010. "edgeR: A Bioconductor Package for Differential Expression Analysis of Digital Gene Expression Data." *Bioinformatics* 26: 139–140.

Sedlak, M., and N. W. Y. Ho. 2004. "Characterization of the Effectiveness of Hexose Transporters for Transporting Xylose During Glucose and Xylose Co-Fermentation by a Recombinant Saccharomyces Yeast." *Yeast* 21: 671–684.

Seppälä, S., K. V. Solomon, S. P. Gilmore, J. K. Henske, and M. A. O'Malley. 2016. "Mapping the Membrane Proteome of Anaerobic Gut Fungi Identifies a Wealth of Carbohydrate Binding Proteins and Transporters." *Microbial Cell Factories* 15: 212.

Shin, H. Y., J. G. Nijland, P. P. de Waal, R. M. de Jong, P. Klaassen, and A. J. M. Driessen. 2015. "An Engineered Cryptic Hxt11 Sugar Transporter Facilitates Glucose-Xylose Co-Consumption in *Saccharomyces cerevisiae*." *Biotechnology for Biofuels* 8: 176.

Steen, E. J., Y. Kang, G. Bokinsky, et al. 2010. "Microbial Production of Fatty-Acid-Derived Fuels and Chemicals From Plant Biomass." *Nature* 463: 559–562.

Su, S., C. W. Law, C. Ah-Cann, M. L. Asselin-Labat, M. E. Blewitt, and M. E. Ritchie. 2017. "Glimma: Interactive Graphics for Gene Expression Analysis." *Bioinformatics* 33: 2050–2052.

Subtil, T., and E. Boles. 2012. "Competition Between Pentoses and Glucose During Uptake and Catabolism in Recombinant *Saccharomyces cerevisiae*." *Biotechnology for Biofuels* 5: 14.

Tani, T., H. Taguchi, and T. Akamatsu. 2017. "Analysis of Metabolisms and Transports of Xylitol Using Xylose- and Xylitol-Assimilating *Saccharomyces cerevisiae*." *Journal of Bioscience and Bioengineering* 123: 613–620.

Thite, V. S., and A. S. Nerurkar. 2019. "Valorization of Sugarcane Bagasse by Chemical Pretreatment and Enzyme Mediated Deconstruction." *Scientific Reports* 9: 15904.

Toivari, M. H., L. Salusjärvi, L. Ruohonen, and M. Penttilä. 2004. "Endogenous Xylose Pathway in *Saccharomyces cerevisiae*." *Applied and Environmental Microbiology* 70, no. 6: 3681–3686.

Tsai, C. S., I. I. Kong, A. Lesmana, et al. 2015. "Rapid and Marker-Free Refactoring of Xylose-Fermenting Yeast Strains With Cas9/CRISPR." *Biotechnology and Bioengineering* 112, no. 11: 2406–2411.

Xue, X., J. Wang, D. Shukla, L. S. Cheung, and L. Q. Chen. 2022. "When SWEETs Turn Tweens: Updates and Perspectives." *Annual Review of Plant Biology* 73: 379–403.

Young, E. M., A. Tong, H. Bui, C. Spofford, and H. S. Alper. 2014. "Rewiring Yeast Sugar Transporter Preference Through Modifying a Conserved Protein Motif." *Proceedings of the National Academy of Sciences* 111: 131–136.

Supporting Information

Additional supporting information can be found online in the Supporting Information section.
Supplementary information_for_ver16.